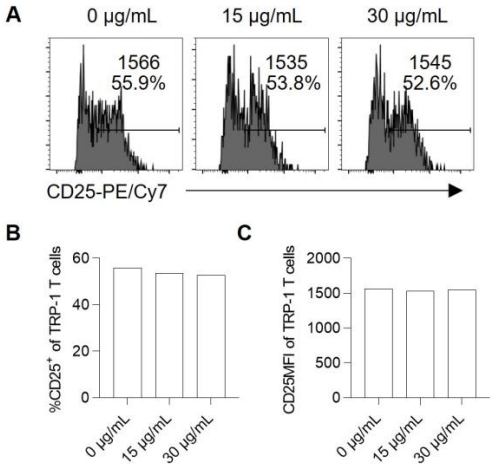

Fig. S1. Binding of mIL-2/CD25 to the IL-2R does not affect detection of cell surface-associated CD25 by CD25 antibody. TRP-1 splenocytes were induced to express the high affinity IL-2R by stimulation with TRP-1 antigen and changes on CD25 mean fluorescence intensity (MFI) were assessed 48 hrs later upon incubation with increasing concentrations of mIL-2/CD25 (0-30 µg/mL) as indicated by staining with CD25(PC61)-PE/Cy7 antibody. (**A**) Representative histograms of CD25 expression on TRP-1 T cells where MFI and percentage are the top and bottom values, respectively. (**B**) Quantification of percent CD25 and (**C**) CD25 MFI on the TRP-1 T cells. Data were obtained from one experiment.

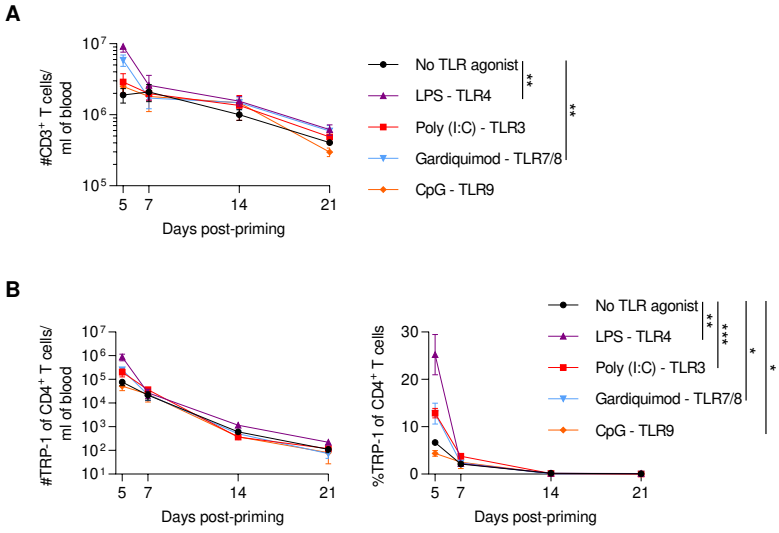

Fig. S2. Optimal TRP-1 Teff expansion by mIL-2/CD25 requires specific TLR signaling. TRP-1 T cells were transferred as described in Fig. 1 and primed with cognate antigen and LPS (10 µg), poly (I:C) (50 µg), gardiquimod (100 µg), or CpG (20 µg), as indicated. High-dose mIL-2/CD25 (100 µg) was administered one day post-priming. (**A**) The numbers of CD3+ T cells in the blood. (**B**) The numbers (left) and frequencies (right) of TRP-1 T cells in the blood. Data (n = 4-5 mice/group) were pooled from two independent experiments and analyzed using an unpaired t test which compares the TLR-treated groups with the no TLR agonist group for day 5 only in (**A**) and (**B**) for % TRP-1.

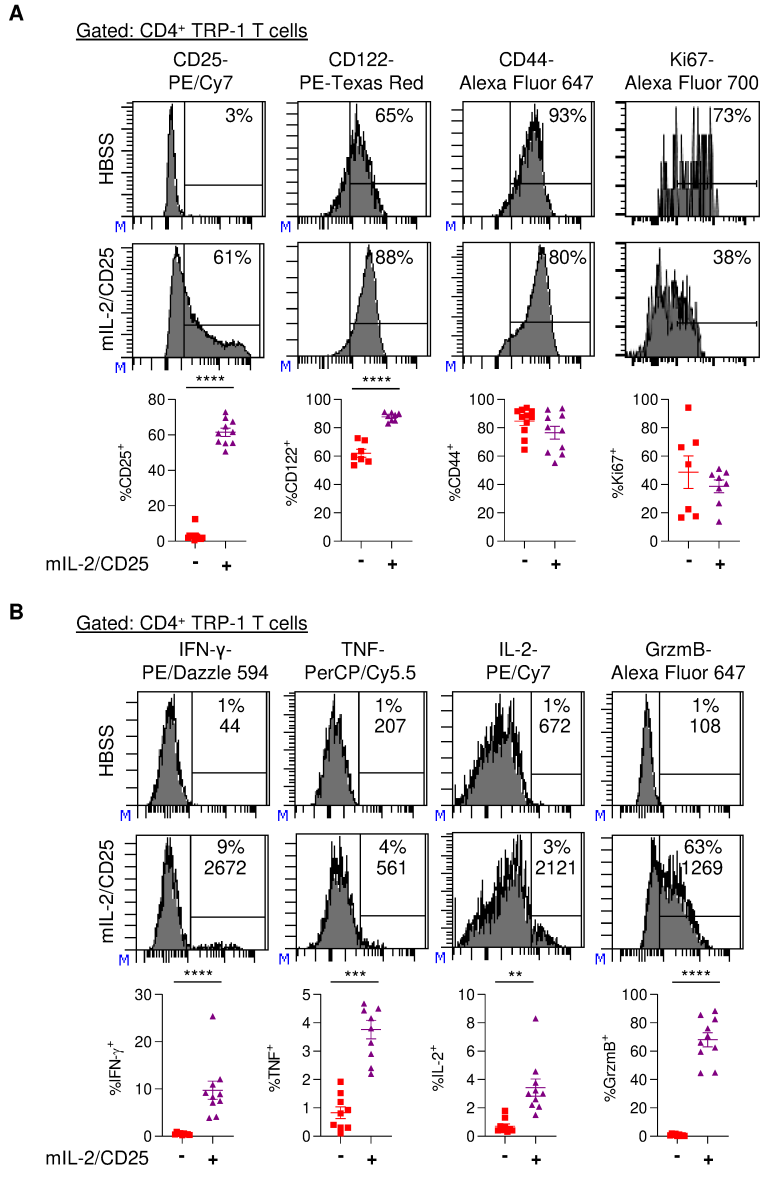

Fig. S3. A single high dose of mIL-2/CD25 enhances TRP-1 activation and function. TRP-1 T cells were transferred and immunized as described in Fig. 1 using mIL-2/CD25 (100 µg). TRP-1 T cells from the spleen were assayed 5 days post-priming. Representative FACS plots (top) and quantitative data (bottom) are shown. (**A**) Markers of T cell activation and proliferation. (**B**) Markers of functional activity after in vitro re-stimulation with TRP-1 peptide. Data (n = 7-11 mice/group) were pooled from two to three independent experiments and analyzed using Welch's unpaired t test.

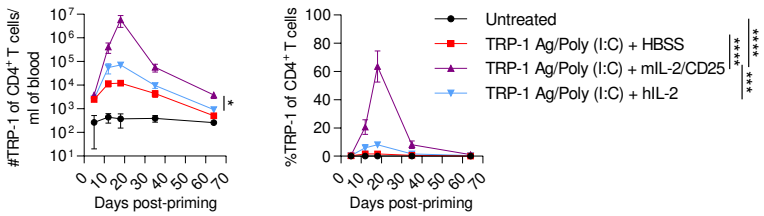

Fig. S4. mIL-2/CD25 administration following antigen boosting immunizations amplifies physiologic numbers of TRP-1 CD4⁺ T cells to higher levels than similar doses of hIL-2. TRP-1 CD4⁺ T cells (3 x 10^3) were transferred as in Fig. 1 and primed with TRP-1 antigen (Ag) and poly (I:C) i.v. on days 0, 7, and 13. mIL-2/CD25 (50 µg) or hIL-2 (12.5 µg) were administered after each boosting immunization. Number (left) and frequency (right) of TRP-1 T cells in the blood at the indicated time. Data (n = 5-8 mice/group) were pooled from two independent experiments and analyzed by ordinary one-way ANOVA and Tukey's test for multiple comparisons where TRP-1 T cell numbers were analyzed for day 64 only comparing mIL-2/CD25 to hIL-2 treatment. Percent data were analyzed by determining the area under curve. Significance values for percent data are shown on the figure key.

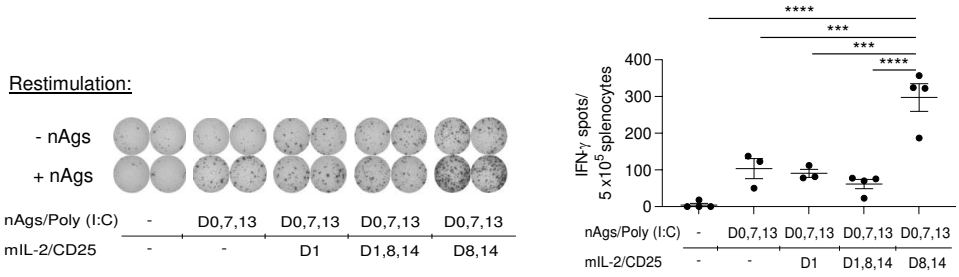

Fig. S5. High-dose mIL-2/CD25 administration after boosting neoantigen vaccinations amplifies neoantigen-specific T cells in tumor-bearing animals. Mice were challenged with B16-F10 on day -3 and immunized with the pool of B16-F10 neoantigens (nAgs) and poly (I:C). mIL-2/CD25 (50 μg) was administered 24 hrs after the initial priming step, boosting steps, or both after priming and boostings with the neoantigen vaccine, as indicated. On day 18 post-priming, splenocytes were in vitro restimulated with or without the B16-F10 nAg pool and IFN-γ ELISpots were determined 24 hrs later. Shown are representative ELISpots (left) and frequency of ELISpots per 5 x 10^5 splenocytes (right). Data (n = 3-4 mice/group) was collected from one experiment and analyzed using ordinary one-way ANOVA and Tukey's test for multiple comparisons.

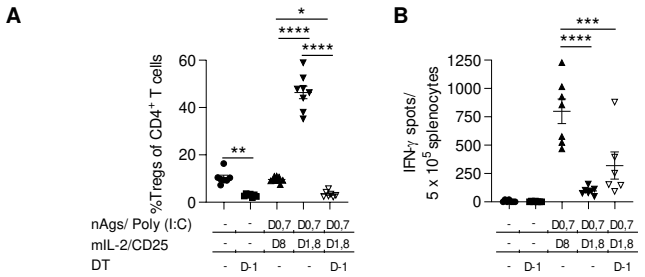

Fig. S6. Treg depletion prior to priming endogenous T cells with neoantigens does not enhance neoantigen-specific T cell expansion. Foxp3^{DTR} mice received diphtheria toxin (DT) (1 μg) prior to the vaccination regimen with neoantigens (nAgs), poly (I:C), and mIL-2/CD25 as shown. (**A**) Frequency of Tregs in the blood on day 4 post priming with the neoantigen vaccine. (**B**) Quantitative data of the number of IFN-γ ELISpots on day 12 post-priming. Data (n = 5-8 mice/group) were pooled from two independent experiments and were analyzed by ordinary one-way ANOVA and Tukey's test for multiple comparisons. Significant figures are only shown for relevant groups, including DT-treated mice compared to untreated mice and vaccinated mice compared to vaccinated mice receiving DT treatment.

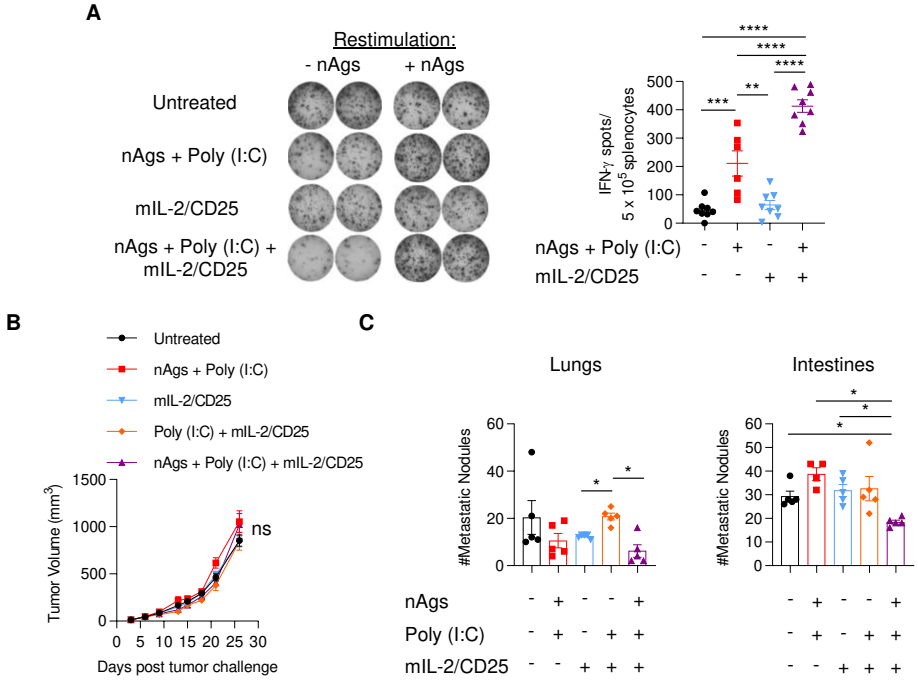
A
Restimulation:
- nAgs
+ nAgs
Untreated
nAgs + Poly (I:C)
mIL-2/CD25
nAgs + Poly (I:C) + mIL-2/CD25
IFN-γ spots/ 5 x 10^5 splenocytes
nAgs + Poly (I:C)
mIL-2/CD25
B
Untreated
nAgs + Poly (I:C)
mIL-2/CD25
Poly (I:C) + mIL-2/CD25
nAgs + Poly (I:C) + mIL-2/CD25
Tumor Volume (mm3)
ns
Days post tumor challenge
C
Lungs
Intestines
#Metastatic Nodules
nAgs
Poly (I:C)
mIL-2/CD25

Fig. S7.

Fig. S7. mIL-2/CD25 increases the frequency of 4T1 neoantigen-specific T cells and reduces 4T1 metastatic nodules in mice vaccinated with MHC class I neoantigens. BALB/c mice were immunized with a pool of 4 MHC class I neoantigens (nAgs) and poly (I:C) (50 μg each). mIL-2/CD25 was administered 24 hrs after the nAg boosting immunization. (**A**) Mice were immunized on days 0 and 7 and received mIL-2/CD25 on day 8. Splenocytes were restimulated with or without nAgs in vitro on day 12 and IFN-γ ELISpots were determined 22-24 hrs post-restimulation. Representative ELISpots (left) and quantitative data (right) normalized to splenocytes which did not receive nAgs restimulation in vitro. Data (n = 6-8 mice/group) were pooled from three independent experiments and analyzed using ordinary one-way ANOVA and Tukey's test for multiple comparisons. (**B** and **C**) Mice were inoculated with 4T1 on day -3 and immunized on days 0, 7, and 13 with nAgs and poly (I:C). mIL-2/CD25 (50 μg) was administered after each boosting immunization. (**B**) Tumor growth curves and (**C**) quantitative data for the number of metastatic nodules in the lungs and intestines assessed 29 days post-priming with the neoantigen vaccine. Data (n = 5-10 mice/group) were pooled from two independent experiments and analyzed by determining the area under curve followed by ordinary one-way ANOVA and Tukey's test for multiple comparisons (**B**), or Welch's ANOVA and Dunnett's T3 test for multiple comparisons (**C**).

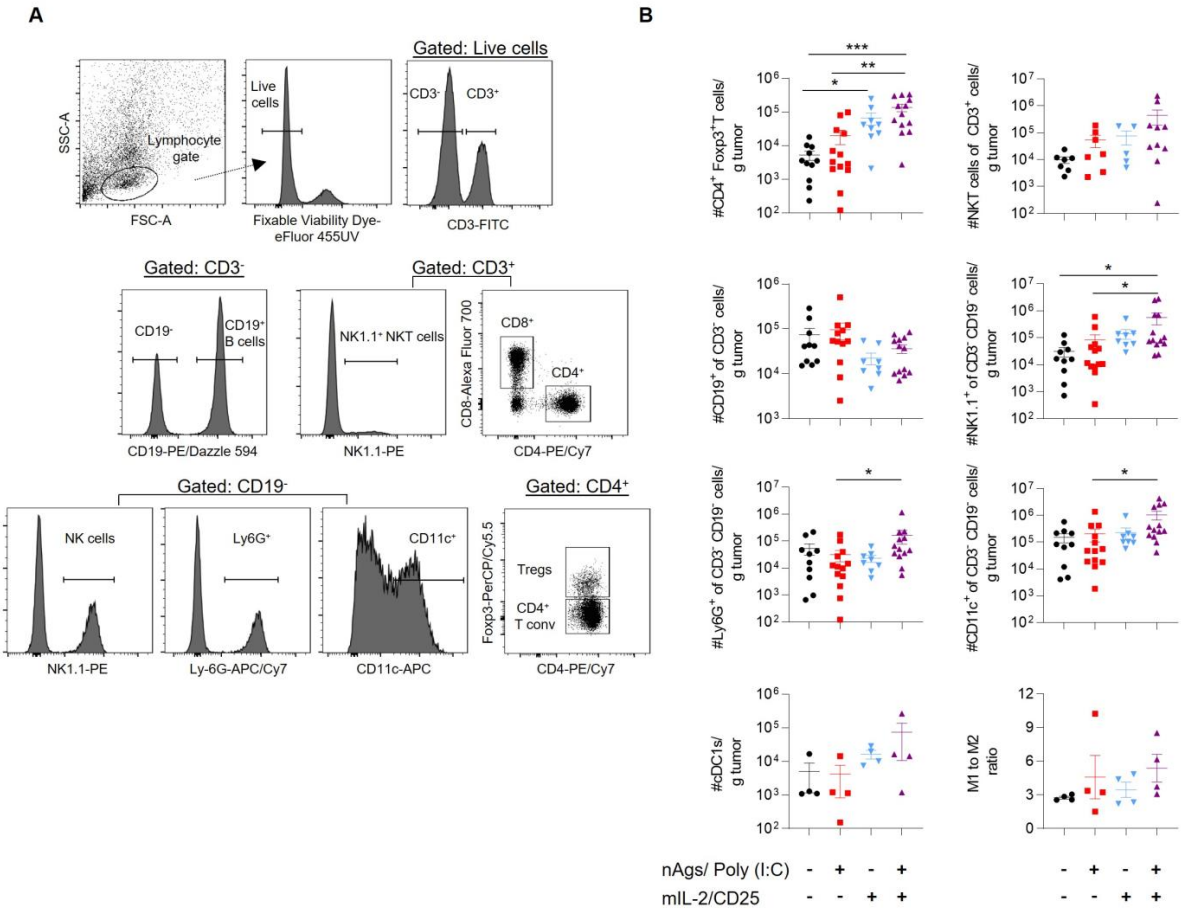

Fig. S8. mIL-2/CD25 as a monotherapy or in combination with the B16-F10 neoantigen vaccine influences the immune composition of the tumor microenvironment. C57BL/6 mice were challenged with B16-F10 and immunized using the regimen described in Fig. 5 C and D. Tumors were assessed on day 18 post-priming. (**A**) Representative gating strategy for tumor-infiltrating immune cells. (**B**) Numbers of tumor infiltrating immune cells per gram of tumor. Data (n = 4-13 mice/group) were pooled from two to three independent experiments or one experiment for conventional type 1 DCs (cDC1s) and M1 and M2 macrophage ratios. All data were analyzed using Kruskal-Wallis test.

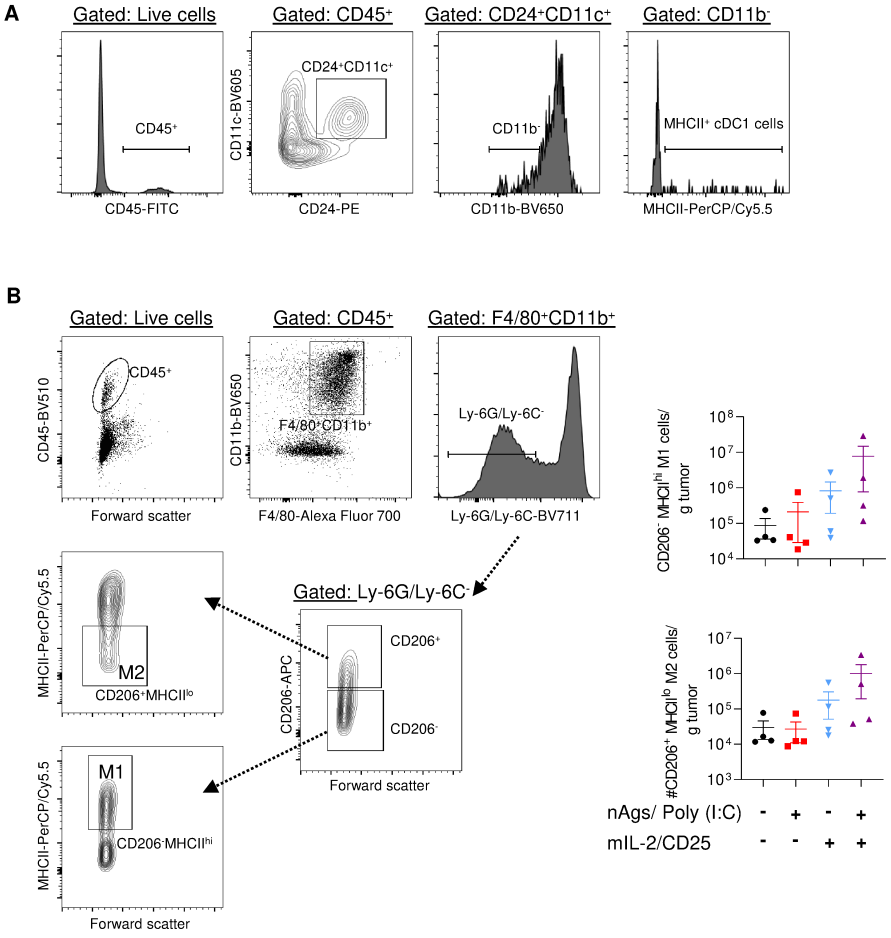

Fig. S9. Gating strategy for the identification of conventional type 1 DCs and macrophage subsets within the tumor microenvironment. C57BL/6 mice were challenged with B16-F10 and immunized using the regimen described in Fig. 5 C and D. Tumors were assessed on day 18 post-priming. (**A**) Gating strategy for the identification of conventional type 1 DCs (cDC1s) quantified in Fig. S8B. (**B**) M1 and M2 macrophage subsets were identified as shown to the left. The numbers per gram of tumor of each subset are shown to the right and were used to determine the M1 to M2 ratio found in Fig. S8B. Data (n = 4 mice/group) were obtained from one experiment and analyzed using Kruskal-Wallis test.

mAb Target	Clone	mAb Label	Source	Staining Concentration	Catalog Number
CD45	30-F11	FITC	BD Pharmingen	2.0 µg/ml	553080
CD45	30-F11	BV510	BioLegend	1.0 µg/ml	103137
CD45.2	104	FITC	BioLegend	4.0 µg/ml	109806
CD3ε	145-2C11	FITC	ThermoFisher	2.5 µg/ml	11-0031-82
CD4	RM4-5	BV510	BioLegend	2.0 µg/ml	100559
CD4	RM4-5	PE/Cy7	BD Pharmingen	0.25 µg/ml	552775
CD8α	53-6.7	Alexa Fluor 700	ThermoFisher	1.0 µg/ml	56-0081-82
CD8α	53-6.7	PerCP/Cy5.5	BioLegend	2.5 µg/ml	100734
Foxp3	FJK-16s	eFluor 450	ThermoFisher	2.0 µg/ml	48-5773-82
Foxp3	FJK-16s	PerCP/Cy5.5	ThermoFisher	1:200 dilution	45-5773-82
NK-1.1	PK136	PE	BD Pharmingen	2.0 µg/ml	553165
CD11b	M1/70	PE/cy7	BioLegend	2.0 µg/ml	101216
CD11b	M1/70	BV650	BioLegend	2.0 µg/ml	101239
CD11c	HL3	Biotin	BD Pharmingen	10.0 µg/ml	553800
CD11c	N418	BV605	BioLegend	2.5 µg/ml	117333
CD19	6D5	PE/Dazzle 594	BioLegend	2.0 µg/ml	115554
Ly-6G	1A8	APC/Cy7	BioLegend	2.0 µg/ml	127624
Ly-6G/Ly-6C	RB6-8C5	BV711	BioLegend	2.0 µg/ml	108443
CD24	30-F1	PE	BioLegend	2.0 µg/ml	138504
F4/80	BM8	Alexa Fluor 700	BioLegend	5.0 µg/ml	123130
CD206	C068C2	Alexa Fluor 647	BioLegend	10.0 µg/ml	141712
pSTAT5	pY694	Alexa Fluor 647	BD Pharmingen	1:10 dilution	612599
CD122	TM-β1	Biotin	BioLegend	10.0 µg/ml	123206
Ki67	B56	Alexa Fluor 700	BD Pharmingen	1:50 dilution	561277
CD44	Pgp-1	Alexa Fluor 647	Laboratory made	5.0 µg/ml	N/A
CD44	IM7	APC/Cy7	BioLegend	1.4 µg/ml	103028
CD25	PC61	PE/Cy7	BD Pharmingen	1.25 µg/ml	552880
CD25	PC61	BV711	BioLegend	2.0 µg/ml	102049
PD-1	RMP1-14	PE	BioLegend	10.0 µg/ml	114118
CTLA-4	UC10-4B9	PE/Cy7	BioLegend	6.0 µg/ml	106314
IFN-γ	XMG1.2	PE/Dazzle 594	BioLegend	2.0 µg/ml	505846
TNF-α	MP6-XT22	PerCP/Cy5.5	BioLegend	2.0 µg/ml	506322
IL-2	JES6-5H4	PE/Cy7	eBioscience	10.0 µg/ml	25-7021-82
Granzyme B	GB11	Alexa Fluor 647	BD Pharmingen	4.0 µg/ml	560212
MHC class I	AF6-88.5	PE	BioLegend	2.0 µg/ml	116507
MHC class II	M5/114.15.2	PerCP/Cy5.5	BioLegend	2.0 µg/ml	107625
Fixable Viability Dye	N/A	eFluor 455UV	ThermoFisher	1:100 dilution	65-0868-18
		Streptavidin Conjugate Label	**Source**	**Staining Concentration**	**Catalog Number**
		PE-Texas Red	BD Pharmingen	2.0 µg/ml	551487
		APC	BioLegend	2.0 µg/ml	405207

Table S1. List of labeled monoclonal antibodies (mAb) and fluorochrome-streptavidin conjugates including source and staining concentrations.